

IMPLICIT NEURAL REPRESENTATION FOR MRI PARALLEL IMAGING RECONSTRUCTION

Hao Li^{1,†}, Yusheng Zhou^{2,†}, Jianan Liu^{3,*}, Xiling Liu⁴, Tao Huang⁵, and Zhihan Lv⁶

¹ The Department of Neuroradiology, University Hospital Heidelberg, Heidelberg, Germany;

² School of Electrical Engineering and Automation, Wuhan University, Wuhan, China;

³ Vitalent Consulting, Gothenburg, Sweden;

⁴ Department of Stomatology, Shenzhen People’s Hospital, Shenzhen, China;

⁵ The College of Science and Engineering, James Cook University, Cairns, Australia;

⁶ Department of Game Design, Faculty of Arts, Uppsala University, Sweden.

ABSTRACT

Magnetic resonance imaging (MRI) always suffers from long acquisition times. Parallel imaging (PI) is one solution to reduce scan time by periodically skipping certain K-space lines and then reconstructing high-quality images from under-sampled measurements. Recently, implicit neural representation (INR) has emerged as a new deep learning method that represents an object as a continuous function of spatial coordinates, and this function is normally parameterized by a multilayer perceptron (MLP). In this paper, we propose a novel MRI PI reconstruction method based on INR, which represents the reconstructed fully-sampled images as the function of voxel coordinates and prior feature vectors of under-sampled images to overcome the generalization problem of INR. Specifically, we introduce a scale-embedded encoder to produce scale-independent voxel-specific features from MR images with different undersampling scales and then concatenate with coordinate vectors to recover fully-sampled MR images, thus achieving multiple scale reconstructions. The performance of the proposed method was assessed by experimenting with publicly available MRI datasets and was compared with other reconstruction methods. Our quantitative evaluation demonstrates the superiority of the proposed method over alternative reconstruction methods.

Index Terms—

Magnetic resonance imaging, parallel imaging reconstruction, implicit neural representation, supervised learning

1. INTRODUCTION

Magnetic resonance imaging (MRI) is a pivotal non-ionizing medical imaging modality. A persistent concern in MRI is

This work has been submitted to the IEEE for possible publication. Copyright may be transferred without notice, after which this version may no longer be accessible.

[†] Authors contribute equally to this work and are co-first authors.

* Corresponding Author, Email: jianan.liu@vitalent.se

the protracted acquisition time. Strategies to enhance MRI acquisition speed while preserving image fidelity entail omitting K-space lines in the phase-encoding direction, followed by image reconstruction from the under-sampled data. Noteworthy methodologies include compressed sensing (CS) [1] and parallel imaging (PI) [2, 3]. PI as the most widely used method to accelerate MRI scans, leverages the redundancy inherent in multiple receiving coil elements to reduce phase encoding steps periodically. Nevertheless, PI is susceptible to noise and aliasing artifacts at high undersampling factors.

Recently, deep learning-based methods have shown great potential in MRI reconstruction tasks. These methods can be divided into two types: data-driven and model-driven [4]. The data-driven methods [5, 6] train end-to-end neural networks for learning the potential mapping from under-sampled MR images to fully-sampled MR images. In contrast, the model-driven methods [7, 8] unroll the conventional reconstruction iterative algorithm and use networks to learn the auxiliary parameters or regularizations. These methods have significantly improved over conventional PI-based methods and achieved impressive performance. However, most of the existing deep learning-based methods are designed to reconstruct MRI with a fixed undersampling scale. They must be trained and stored for each scale factor, which is highly computationally expensive and resource-intensive.

Over the past years, implicit neural representation (INR) has emerged with rising popularity for various tasks in computer vision. It is designed to model the 2D slice or 3D volume as a continuous function of spatial coordinates and parameterize the function [9]. A well-known INR-based work proposed by Mildenhall *et al.* [10] is the neural radiance fields (NeRF), which represent a scene by a fully connected deep network to render novel views with impressive visual quality. Besides, INR has also been applied to medical image tasks. An INR-based super-resolution framework was proposed to upsample the MRI image volume at arbitrary scales in a continuous domain [11, 12]. NeRP [13] reconstructed static MRI

from sparsely sampled k-space data with prior embedding. NeSVoR [14] reconstructed MR volume from a slice based on INR. All of this work has yielded interesting results. However, the main drawback is to train a specific network for each image slice, resulting in hours for each subject [15], which is time-consuming and impractical in real clinics.

Inspired by these INR-based works, we adopted INR for the reconstruction of MRI PI to overcome the generalization problems of conventional INR approaches, such as the subject-specific and undersampling factor-specific constraints. The main contributions of this paper include:

- An implicit neural representation (INR) approach is proposed to represent fully-sampled MRI images as a continuous function of spatial coordinates and prior voxel-specific features of undersampled MRI.
- We introduce a convolutional encoder network to produce voxel-specific features from the undersampled MRI images as additional prior information input to the implicit function, thus recovering voxel intensities without subject-specific constraints.
- The encoder is embedded with a reconstruction scale for generating uniform scale-independent features, which enables the implicit function to recover MRI with multiple undersampling scales, with which the network is not even trained.
- Experimental results showed that compared with other MRI PI reconstruction methods, our method obtained improved performance and generated superior-quality images.

2. METHODOLOGY

2.1. Problem Formulation

For an MRI system, the undersampled k-space signal y can be expressed as:

$$y = \mathbf{A}I + \mathbf{n} \quad (1)$$

where I represents the image to be reconstructed and \mathbf{n} is the measurement noise. $\mathbf{A} = \mathbf{M}\mathbf{F}$ denotes the degradation operator, where \mathbf{M} is a sampling mask and \mathbf{F} denotes the Fourier transform. In previous MRI reconstruction studies, the image I is restored by minimizing the following objective function:

$$\operatorname{argmin}_I \frac{1}{2} \|y - \mathbf{A}I\|^2 \quad (2)$$

In INR, the MRI intensities I is regarded as a continuous coordinated-based implicit function, i.e., $f_\theta(\mathbf{x})$, where θ indicates the parameters of this function and $\mathbf{x} = (x, y)$ denotes 2D voxel coordinates, which are normalized to the range of $[-1, 1]$. Let I_θ be the discretized image matrix after uniform sampling from f_θ at the voxel locations. In this case, the reconstruction objective is rewritten as:

$$\operatorname{argmin}_\theta \frac{1}{2} \|y - \mathbf{A}I_\theta\|^2 \quad (3)$$

Based on implicit neural representation (INR), f_θ is built as a multilayer perceptron (MLP). Thus, this reconstruction problem is transformed into training a network to optimize function (3).

2.2. Arbitrary Scale Reconstruction

To improve the learning of high-frequency features, we adopt a positional encoding method from Tancik *et.al.* [16]. The coordinates $\mathbf{x} \in \mathbb{R}^2$ are mapped to a higher dimension space \mathbb{R}^{2L} using an encoding function γ before passing to the MLP:

$$\gamma(\mathbf{x}) = [\cos(2\pi B\mathbf{x}), \sin(2\pi B\mathbf{x})]^T \quad (4)$$

where B represents the encoding coefficients. All entries of matrix B are sampled from the Gaussian distribution $\mathcal{N}(\mathbf{0}, \sigma^2)$, where σ is a tunable hyperparameter. In this work, σ is set to 1.

Training a specific function f_θ for each undersampled image is impractical in clinical settings. Instead, a generic one is preferred. Towards this end, the prior intensity information of the undersampled images is used as an extra input of f_θ , due to the lack of specificity of coordinates. We induce a convolutional encoder network to compress the local voxel intensity of the input images into a voxel-specific feature map $V \in \mathbb{R}^{h \times w \times d}$. Thus, each feature vector in the feature map denoted by $v_{\mathbf{x}} \in \mathbb{R}^d$ contains the local semantic information of the MR image at the coordinate \mathbf{x} , which helps MLP recover the specific voxel intensity.

Furthermore, the undersampling scale of each MRI is not limited to a specific value in this recovery process, which means the implicit function f_θ only learns the mapping from coordinates and feature vectors to voxel intensities. Thus, a reconstruction of multiple scale factors can be theoretically achieved. To enable the ability to discriminate different reconstruction scales and generate a uniform scale-independent feature map, we also embed the scale factor into the encoder.

$$v_{\mathbf{x}}^s = \text{Encoder}(I_u^s, s)(\mathbf{x}) \quad (5)$$

where s is the reconstruction scale, I_u^s is the undersampled MR images with the reconstruction scale s , and $v_{\mathbf{x}}^s$ denotes the prior feature vector of image I_u^s at the coordinate \mathbf{x} .

Finally, the implicit voxel function is:

$$I = f_\theta(\gamma(\mathbf{x}), v_{\mathbf{x}}^s) \quad (6)$$

f_θ and scale-embedded encoder are trained at the same time, and the MRI images with multiple undersampling scales can be reconstructed in a short time after the training.

Since all the operations mentioned above are conducted in the image domain, we modify the reconstruction objective for convenient training of all networks:

$$\operatorname{argmin}_\theta \frac{1}{2} \|I^* - I_\theta\|^2 \quad (7)$$

where I^* denotes the fully-sampled MR image.

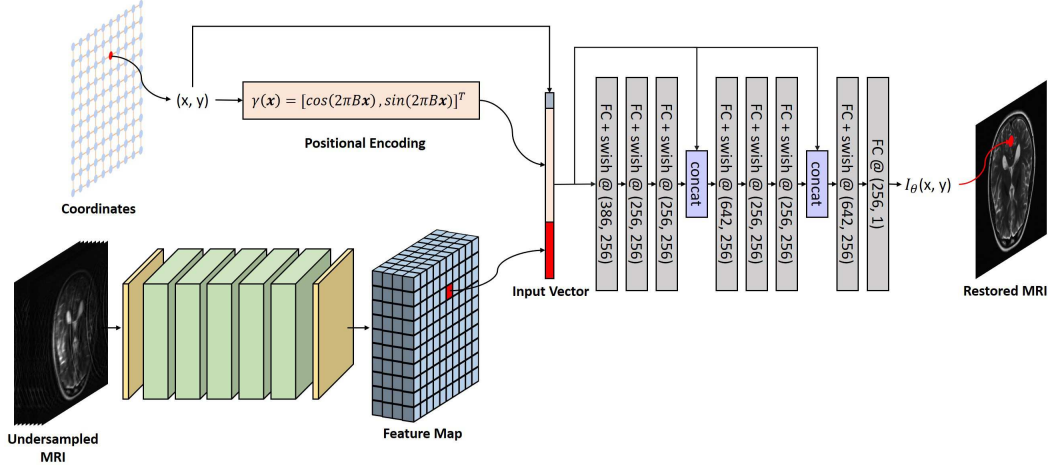


Fig. 1. The workflow of the proposed model. The undersampled images acquired with the multi-channel coil are first converted into a feature map through a scale-embedded encoder, while the 2D voxel coordinates in the MRI grid are mapped into higher-dimension vectors. The feature vectors and the coordinates vectors are concatenated at each coordinate and fed into MLP to recover voxel intensities at each corresponding coordinate.

2.3. Overall Framework

The overall framework of our method is illustrated in Fig. 1. We first convert the undersampled images into a feature map through a convolutional encoder network with reconstruction-scale embedding. The undersampled images are fed into the encoder both with and without the pre-combination of multi-channel images. In the meantime, the 2D voxel coordinates (x, y) of the MR image grid are mapped into higher-dimension vectors. The feature vectors and the coordinate vectors are concatenated at each coordinate and fed into MLP to recover voxel intensities at each corresponding coordinate. During training, the encoder and MLP are simultaneously optimized by minimizing the L1 loss between I^* and I_θ .

Specifically, the convolutional encoder network contains five scale-embedded residual blocks; all convolutional layers have 5x5-sized kernels for a large receptive field and 64 feature channels. We apply the group normalization [17] and use the SWISH [18] as our activation function. The positional encoding dimension $2L$ is set to 256, while the dimension d of feature vectors is 128. For MLP, the network has eight fully connected layers. A SWISH activation follows all layers but the last. Besides, we include two skip connections that concatenate the input of the network to the 4th and 7th layers, respectively. Except that there are $2L + d$, $2L + d + 256$, and $2L + d + 256$ neurons in the 1st, 4th, and 7th layers, others have all 256 neurons.

3. EXPERIMENTS AND RESULTS

3.1. Implementation Details

All our experiments were implemented on a workstation with 64GB RAM and two NVIDIA GeForce RTX 2080 Ti graph-

ics cards. Pytorch 1.8.1 was used as the back end. We trained our model for 100000 iterations using the ADAM optimizer with $\beta_1 = 0.9$, $\beta_2 = 0.99$, and set the batch size to 2. The initial learning rate was set to 0.001 and dropped by half every 10000 iterations.

3.2. Dataset Description

Two types of MRI data from the fastMRI dataset [21] were used in this study. One type is the fully-sampled 15-channel knee k-space data, which was acquired using the 2D turbo spin-echo sequence without fat suppression. The other one is the fully-sampled T2-weighted 16-channel brain k-space data with 3T field strength. The oversampled region of raw data in the image domain has been removed in our case. All selected datasets were uniformly undersampled with different reconstruction scales and 8% of the central region was reserved as auto-calibration signal (ACS) lines.

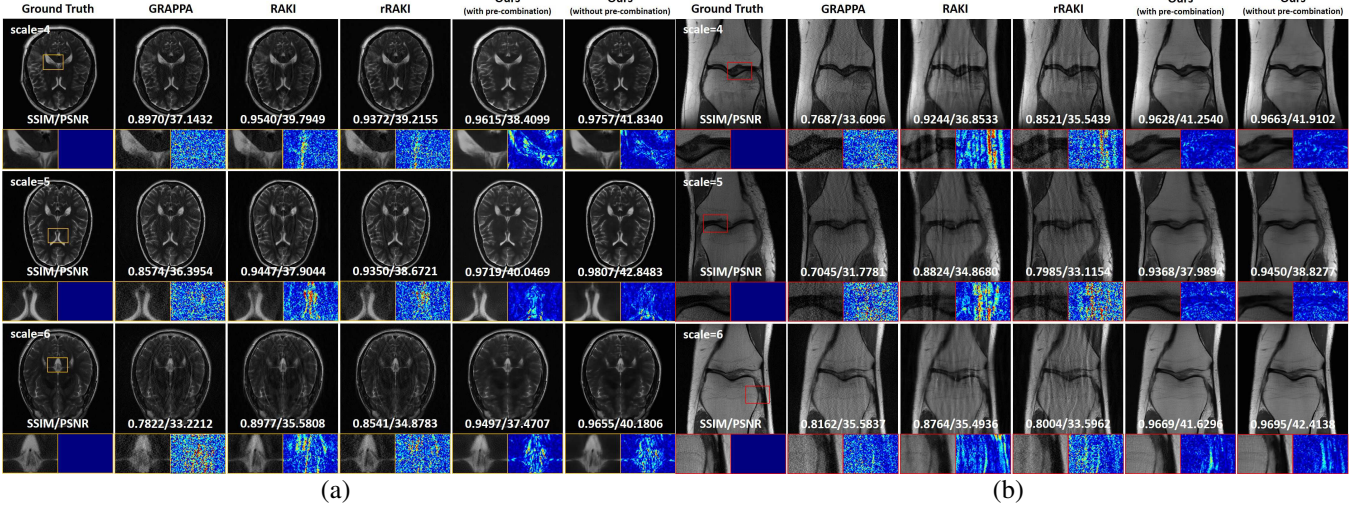
3.3. Experimental Results

In our experiments, we compared the proposed method with GRAPPA [3], RAKI [19], residual RAKI (rRAKI) [20], and Feng *et.al.* [15] on two datasets with reconstruction scales of 4, 5, and 6. Table 1 shows the quantitative evaluation results. We observe that the proposed method with pre-combination of multi-channel images is significantly superior to all comparison methods, and the results of the proposed method without the pre-combination are further improved.

Fig. 2(a) visualizes the reconstruction effects of different methods on the three undersampling scales of the brain dataset. We can observe that these GRAPPA-reconstructed MR images are heavily noisy and suffer from obvious artifacts at higher reconstruction scales. In contrast, RAKI's

Table 1. Quantitative comparison with other parallel reconstruction methods on the fastMRI dataset (**Best** and **Second Best**).

	Brain			Knee		
	$s = 4$	$s = 5$	$s = 6$	$s = 4$	$s = 5$	$s = 6$
GRAPPA [3]	0.8876/36.8103	0.8443/35.5809	0.7921/33.1173	0.7513/32.7750	0.6854/31.4585	0.7930/34.2945
RAKI [19]	0.9501/39.4045	0.9415/38.1688	0.8942/35.0135	0.9169/36.7898	0.8782/34.7770	0.8642/34.3090
rRAKI [20]	0.9317/38.9997	0.9222/38.0567	0.8450/33.9112	0.8440/35.2438	0.7769/32.6516	0.7739/32.3304
Feng <i>et. al.</i> [15]	<i>N/A</i>	<i>N/A</i>	<i>N/A</i>	0.9321/39.4900	0.9296/39.0400	<i>N/A</i>
Ours (with pre-combination)	0.9543/37.7673	0.9624/39.1054	0.9461/36.8490	0.9480/39.4207	0.9406/38.8031	0.9532/39.8919
Ours (without pre-combination)	0.9641/40.5916	0.9664/40.9975	0.9559/39.0309	0.9532/40.1727	0.9458/39.5118	0.9557/40.3630

**Fig. 2.** Comparison of the qualitative performance of the proposed method and GRAPPA, RAKI, and rRAKI.

results have low noise levels and significantly improved SSIM and PSNR; however, the artifacts remain a serious unresolved problem. The performance of rRAKI, including the quality of reconstructed images and evaluation metrics, is between GRAPPA and RAKI. The reconstruction effect of the three methods decreases sharply with the increase in the undersampling scale. On the contrary, the proposed method is more robust, produces similar image quality at different undersampling scales without noise and obvious artifacts, and outperforms the compared methods.

The reconstruction results of different methods conducted on the knee dataset are shown in Fig.2(b). Similar to the experimental results on the brain dataset, GRAPPA, RAKI, and rRAKI still suffer from artifacts and noise. Furthermore, the images reconstructed by RAKI and rRAKI are more blurry, with the boundaries between different tissues over-smoothed. Contrarily, the proposed method successfully reduces noise and artifacts that are apparent in the results of the compared methods, as illustrated by the zoomed-in images in Fig.2(b), and restores images with both high-definition detail and improved image contrast.

4. CONCLUSION

In this paper, we propose an INR-based MRI parallel imaging reconstruction framework. Instead of learning the mapping

from undersampled to fully-sampled MRI under a fixed reconstruction scale directly, we propose to learn a continuous implicit neural voxel function, which takes the higher-dimensional coordinate vectors and the scale-independent voxel-specific features generated by a convolutional scale-embedded encoder network as input to recover voxel intensities at each corresponding coordinate, thereby restoring high-quality MRI. Once the training of the networks for the proposed method is completed, it does not restrict the application to a specific subject or undersampling scale for MRI parallel imaging reconstruction. Our experimental results conducted on three different reconstruction scales show that the proposed method generates images with higher evaluation metrics and enhanced visual quality compared to the baseline models, making it potential for further accelerating the acquisition of MRI.

Despite the superior quality of MRI parallel reconstruction, we acknowledge some limitations with our method. Firstly, the experiments in this paper only verify our model with three different undersampling scales. More scales of MRI reconstruction and more types of MRI data are expected in future studies. Besides, the proposed method was trained in a supervised manner and relied on fully-sampled and undersampled image pairs, which are difficult to obtain in real clinics [22, 23]. Therefore, an unsupervised approach based on the proposed method remains to be investigated.

5. REFERENCES

- [1] Michael Lustig, David Donoho, and John M Pauly, "Sparse MRI: The application of compressed sensing for rapid mr imaging," *Magnetic Resonance in Medicine: An Official Journal of the International Society for Magnetic Resonance in Medicine*, vol. 58, no. 6, pp. 1182–1195, 2007.
- [2] Klaas P Pruessmann, Markus Weiger, Markus B Scheidegger, and Peter Boesiger, "SENSE: Sensitivity encoding for fast mri," *Magnetic Resonance in Medicine: An Official Journal of the International Society for Magnetic Resonance in Medicine*, vol. 42, no. 5, pp. 952–962, 1999.
- [3] Mark A Griswold, Peter M Jakob, Robin M Heidemann, Mathias Nittka, Vladimir Jellus, Jianmin Wang, Berthold Kiefer, and Axel Haase, "Generalized autocalibrating partially parallel acquisitions (GRAPPA)," *Magnetic Resonance in Medicine: An Official Journal of the International Society for Magnetic Resonance in Medicine*, vol. 47, no. 6, pp. 1202–1210, 2002.
- [4] Gushan Zeng, Yi Guo, Jiaying Zhan, Zi Wang, Zongying Lai, Xiaofeng Du, Xiaobo Qu, and Di Guo, "A review on deep learning mri reconstruction without fully sampled k-space," *BMC Medical Imaging*, vol. 21, no. 1, pp. 195, 2021.
- [5] Shanshan Wang, Zhenghang Su, Leslie Ying, Xi Peng, Shun Zhu, Feng Liang, Dagan Feng, and Dong Liang, "Accelerating magnetic resonance imaging via deep learning," in *2016 IEEE 13th international symposium on biomedical imaging (ISBI)*. IEEE, 2016, pp. 514–517.
- [6] Mehmet Akçakaya, Steen Moeller, Sebastian Weingärtner, and Kâmil Uğurbil, "Scan-specific robust artificial-neural-networks for k-space interpolation (RAKI) reconstruction: Database-free deep learning for fast imaging," *Magnetic Resonance in Medicine*, vol. 81, no. 1, pp. 439–453, 2019.
- [7] Hemant K Aggarwal, Merry P Mani, and Mathews Jacob, "MoDL: Model-based deep learning architecture for inverse problems," *IEEE transactions on medical imaging*, vol. 38, no. 2, pp. 394–405, 2018.
- [8] Jian Sun, Huibin Li, Zongben Xu, et al., "Deep admm-net for compressive sensing mri," *Advances in neural information processing systems*, vol. 29, 2016.
- [9] Zhiqin Chen and Hao Zhang, "Learning implicit fields for generative shape modeling," in *Proceedings of the IEEE/CVF Conference on Computer Vision and Pattern Recognition*, 2019, pp. 5939–5948.
- [10] Ben Mildenhall, Pratul P Srinivasan, Matthew Tancik, Jonathan T Barron, Ravi Ramamoorthi, and Ren Ng, "Nerf: Representing scenes as neural radiance fields for view synthesis," *Communications of the ACM*, vol. 65, no. 1, pp. 99–106, 2021.
- [11] Qing Wu, Yuwei Li, Lan Xu, Ruiming Feng, Hongjiang Wei, Qing Yang, Boliang Yu, Xiaozhao Liu, Jingyi Yu, and Yuyao Zhang, "IREM: High-resolution magnetic resonance image reconstruction via implicit neural representation," in *Medical Image Computing and Computer Assisted Intervention—MICCAI 2021: 24th International Conference, Strasbourg, France, September 27–October 1, 2021, Proceedings, Part VI 24*. Springer, 2021, pp. 65–74.
- [12] Zixuan Chen, Jianhuang Lai, Lingxiao Yang, and Xiaohua Xie, "CuNeRF: Cube-based neural radiance field for zero-shot medical image arbitrary-scale super resolution," *arXiv preprint arXiv:2303.16242*, 2023.
- [13] Liyue Shen, John Pauly, and Lei Xing, "NeRP: implicit neural representation learning with prior embedding for sparsely sampled image reconstruction," *IEEE Transactions on Neural Networks and Learning Systems*, 2022.
- [14] Junshen Xu, Daniel Moyer, Borjan Gagoski, Juan Eugenio Iglesias, P Ellen Grant, Polina Golland, and Elfar Adalsteinsson, "NeSVoR: Implicit neural representation for slice-to-volume reconstruction in mri," *IEEE Transactions on Medical Imaging*, 2023.
- [15] Ruimin Feng, Qing Wu, Yuyao Zhang, and Hongjiang Wei, "A scan-specific unsupervised method for parallel mri reconstruction via implicit neural representation," in *2023 IEEE 20th International Symposium on Biomedical Imaging (ISBI)*. IEEE, 2023, pp. 1–5.
- [16] Matthew Tancik, Pratul Srinivasan, Ben Mildenhall, Sara Fridovich-Keil, Nithin Raghavan, Utkarsh Singhal, Ravi Ramamoorthi, Jonathan Barron, and Ren Ng, "Fourier features let networks learn high frequency functions in low dimensional domains," *Advances in Neural Information Processing Systems*, vol. 33, pp. 7537–7547, 2020.
- [17] Yuxin Wu and Kaiming He, "Group normalization," in *Proceedings of the European conference on computer vision (ECCV)*, 2018, pp. 3–19.
- [18] Prajit Ramachandran, Barret Zoph, and Quoc V Le, "Swish: A self-gated activation function," *arXiv preprint arXiv:1710.05941*, vol. 7, no. 1, pp. 5, 2017.
- [19] Mehmet Akçakaya, Steen Moeller, Sebastian Weingärtner, and Kâmil Uğurbil, "Scan-specific robust artificial-neural-networks for k-space interpolation (RAKI) reconstruction: Database-free deep learning for fast imaging," *Magnetic resonance in medicine*, vol. 81, no. 1, pp. 439–453, 2019.
- [20] Chi Zhang, Steen Moeller, Omer Burak Demirel, Kâmil Uğurbil, and Mehmet Akçakaya, "Residual RAKI: A hybrid linear and non-linear approach for scan-specific k-space deep learning," *NeuroImage*, vol. 256, pp. 119248, 2022.
- [21] Florian Knoll, Jure Zbontar, Anuroop Sriram, Matthew J. Muckley, Mary Bruno, Aaron Defazio, Marc Parente, Krzysztof J. Geras, Joe Katsnelson, Hersh Chandarana, Zizhao Zhang, Michal Drozdal, Adriana Romero, Michael Rabbat, Pascal Vincent, James Pinkerton, Duo Wang, Nafissa Yakubova, Erich Owens, C. Lawrence Zitnick, Michael P. Recht, Daniel K. Sodickson, and Yvonne W. Lui, "fastMRI: A publicly available raw k-space and dicom dataset of knee images for accelerated mr image reconstruction using machine learning," *Radiology: Artificial Intelligence*, vol. 2, no. 1, pp. e190007, 2020, PMID: 32076662.
- [22] Jianan Liu, Hao Li, Tao Huang, Euijoon Ahn, Adeel Razi, and Wei Xiang, "Unsupervised representation learning for 3d mri super resolution with degradation adaptation," *arXiv preprint arXiv:2205.06891*, 2022.
- [23] Yusheng Zhou, Hao Li, Jianan Liu, Zhengmin Kong, Tao Huang, Euijoon Ahn, and Zhihan Lv, "UNAEN: Unsupervised abnormality extraction network for mri motion artifact reduction," *arXiv preprint arXiv:2301.01732*, 2023.